Mathematics and Computation, Supercomputing, Reactor Physics and Nuclear and Biological Applications
Palais des Papes, Avignon, France, September 12-15, 2005, on CD-ROM, American Nuclear Society, LaGrange Park, IL (2005)

VENUS-2 MOX-FUELLED REACTOR DOSIMETRY BENCHMARK CALCULATIONS AT VTT

Petri Kotiluoto and Frej Wasastjerna
VTT Technical Research Centre of Finland
P.O. Box 1608, FI-02044 VTT, Finland
petri.kotiluoto@vtt.fi; frej.wasastjerna@vtt.fi

ABSTRACT

VTT, the Technical Research Centre of Finland, has participated in to the on-going international blind benchmark on 3-D VENUS-2 MOX-fuelled reactor dosimetry calculations with the deterministic discrete-ordinate code TORT and the stochastic Monte Carlo code MCNP. Calculations have also been performed by in-house code MultiTrans, which is a deterministic 3-D radiation transport code under development. For both deterministic transport codes, the BUGLE-96 cross-section library was used. MCNP cross-sections were taken from the endf60 library based on ENDF/B-VI. For calculation of ^{58}Ni(n,p), ^{115}In(n,n'), ^{103}Rh(n,n'), ^{64}Zn(n,p), ^{237}Np(n,f), and ^{27}Al(n,α) responses, the IRDF-90 version 2 dosimetry cross-section library was used. With MCNP, this data was directly utilised in the SAND-II scheme, but for deterministic codes the data was condensed into the 47 BUGLE neutron groups. Corresponding fission flux values have been calculated for all the VENUS-2 detector positions. The comparison of the calculated fission fluxes between TORT and MCNP shows rather good agreement: 75 % of the values agree within 10 %. The maximum difference between TORT and MCNP results is 26 % for fission flux values of the ^{27}Al(n,α) reaction inside the water gap. The MultiTrans results, on the other hand, show very large discrepancies inside the neutron pad when compared to the other codes, with 32 % maximum difference between MultiTrans and TORT, and 40 % between MultiTrans and MCNP. The disagreement inside the neutron pad was to some extent anticipated due to more approximative radiation transport method used in MultiTrans. The measured values are at the moment not yet open to the participants, and a comparative analysis between the calculated and measured values will remain as a future work.

KEYWORDS: MCNP, TORT, MultiTrans, VENUS-2

1. INTRODUCTION

At VTT, the Technical Research Centre of Finland, several different radiation transport codes are installed and routinely used for radiation transport problems. Such codes are, for instance, the stochastic Monte Carlo code MCNP [1] and the deterministic 3-D discrete-ordinate code TORT [2]. A new deterministic radiation transport code, MultiTrans, has also been developed at VTT, based on a simplified spherical harmonics approximation of the radiation transport combined with an efficient tree multigrid technique [3–5].

The Nuclear Energy Agency (NEA) of the Organisation for Economic Co-operation and Development (OECD) has been preparing benchmarks related to the use of mixed-oxide (MOX) uranium and plutonium fuel. The on-going benchmark on the 3-D VENUS-2 MOX-fuelled reactor dosimetry calculations is an international blind benchmark with the goal of testing the current state-of-the-art 3-D neutron transport computation methods, especially with MOX-fuelled systems [6]. An objective of participating in the VENUS-2 benchmark has been to further validate our computational systems in routine use, and also to test methods under development, such as the new in-house code MultiTrans.

In this paper we report the computational 3-D VENUS-2 MOX-fuelled benchmark results for TORT, MultiTrans, and MCNP version 4C. This benchmark exercise was performed as a blind test. The measured values are at the moment not yet open to the participants, and therefore a comparative analysis between the calculated and measured values will remain as a future work. However, the comparison of the calculated results between the MultiTrans and the other two codes has possibly revealed some bugs in the MultiTrans code that will require further studying.

2. MATERIALS AND METHODS

2.1. VENUS-2 Benchmark

The Vulcain Experimental NUclear Study (VENUS) facility is a zero power critical reactor located at SCK•CEN in Mol, Belgium. The VENUS-2 core is comprised of 12 “15×15” subassemblies and is characterized by three regions: an inner region with 3.0 w/o enriched UO_2, an outer region with 4.0 w/o enriched UO_2, and a MOX region with 2.0 w/o UO_2 and 2.7 w/o Pu. The measurement positions in VENUS-2 are located along the core-midplane at 34 locations in the outer core region, the core baffle, the water reflector, the core barrel, and the neutron pad. A detailed document of the benchmark specifications, including dimensions and material data of each component, is available from NEA [6].

2.2. Calculations with the Deterministic Codes

For both deterministic codes (TORT and MultiTrans) all material regions were modelled in detail, except that fuel pin, fuel cladding, and water regions were homogenized over each fuel zone. The external regions outside the jacket inner wall (air, jacket outer wall, reactor vessel, water, and reactor room) were omitted from the model, as they can be assumed to have no significant effect to the responses at the measurement points.

The BUGLE-96 cross-section library [7] with 47 neutron groups (with 26 groups above 0.1 MeV) were used for both codes with Legendre order 3 and without upscattering. For the TORT code, the macroscopic cross sections for compound materials were mixed by using TOPICS-B cross-section preparation program [8]. For MultiTrans, the elemental atomic densities were input for each material, and the mixing of the BUGLE cross-sections was done by MultiTrans.

A fixed neutron source was not separately generated: a direct k-effective search (with BUGLE library and homogenised core as explained above) was performed by both codes instead. ^{235}U and ^{239}Pu fission spectra from the BUGLE library were used, weighted by the relative portions of the main fissile isotopes in the VENUS-2 core: $\chi = 0.7930\times\chi(^{235}U) + 0.2070\times\chi\ (^{239}Pu)$. The reference fission rate was given as 4.596E+12 fissions/sec/core quadrant, and by using values of $\nu(^{235}U) = 2.432$ and $\nu\ (^{239}Pu) = 2.8815$ neutrons released per fission event, a normalisation factor (the XNF entry for TORT) of 4.596E+12× (0.7930×2.432+0.2070×2.8815) = 1.161E+13 fission neutrons/sec/core quadrant at 100 % VENUS-2 power was derived.

The International Reactor Dosimetry File (IRDF) was used in calculation of dosimetry responses. IRDF-90 version 2 dosimetry cross-sections for reactions ^{58}Ni(n,p), ^{115}In(n,n'), ^{103}Rh(n,n'), ^{64}Zn(n,p), ^{237}Np(n,f), and ^{27}Al(n,α) were condensed into the BUGLE energy group structure from the SAND-II energy group structure (640 groups) by using X333 utility program from the neutron metrology file NMF-90 [9]. Combined Maxwell, 1/E, and fission weighting spectrum was used. The fission spectrum averaged dosimetry cross-sections are given in Table I. The fission spectrum averaging of the cross-sections in BUGLE multigroup structure has been performed according to Eq. 1.

$$< \sigma_i >_{fiss.} = \frac{\sum_{g=1}^{47} \chi_5^g \sigma_i^g}{\sum_{g=1}^{47} \chi_5^g} \tag{1}$$

In Eq. 1 above, χ_5^g is the fission spectrum in BUGLE neutron groups $g \in [1,47]$ and σ_i^g is the corresponding cross-section of the reaction *i* condensed into the same energy group structure.

Table I. Fission spectrum averaged dosimetry cross-sections

Reaction	**^{58}Ni(n,p)**	**^{115}In(n,n')**	**^{103}Rh(n,n')**	**^{64}Zn(n,p)**	**^{237}Np(n,f)**	**^{27}Al(n,α)**
Cross-section [mbarn]	107.339	187.544	708.720	39.024	1357.720	0.747

2.2.1. TORT discrete-ordinate code

TORT is a 3-D deterministic neutron and photon radiation transport code developed in Oak Ridge. It is based on the well-known discrete-ordinate transport approximation. TORT supports both cylindrical and Cartesian geometry models.

In VENUS-2 calculations, a fully symmetrical S_8 quadrature set was utilised with Legendre order P_3 representation for the angular flux. The geometry input for the TORT code was prepared by using BOT3P [10,11]: a 147R×98Θ×45Z TORT mesh was created. The BOT3P model and the corresponding TORT mesh at the core mid-plane are shown in Figure 1.

The TORT calculations were performed on an AlphaServer ES45 unix workstation with 4 EV6.8CB 1.0 GHz processors: the problem cpu time for a criticality calculation was 18.7 hours.

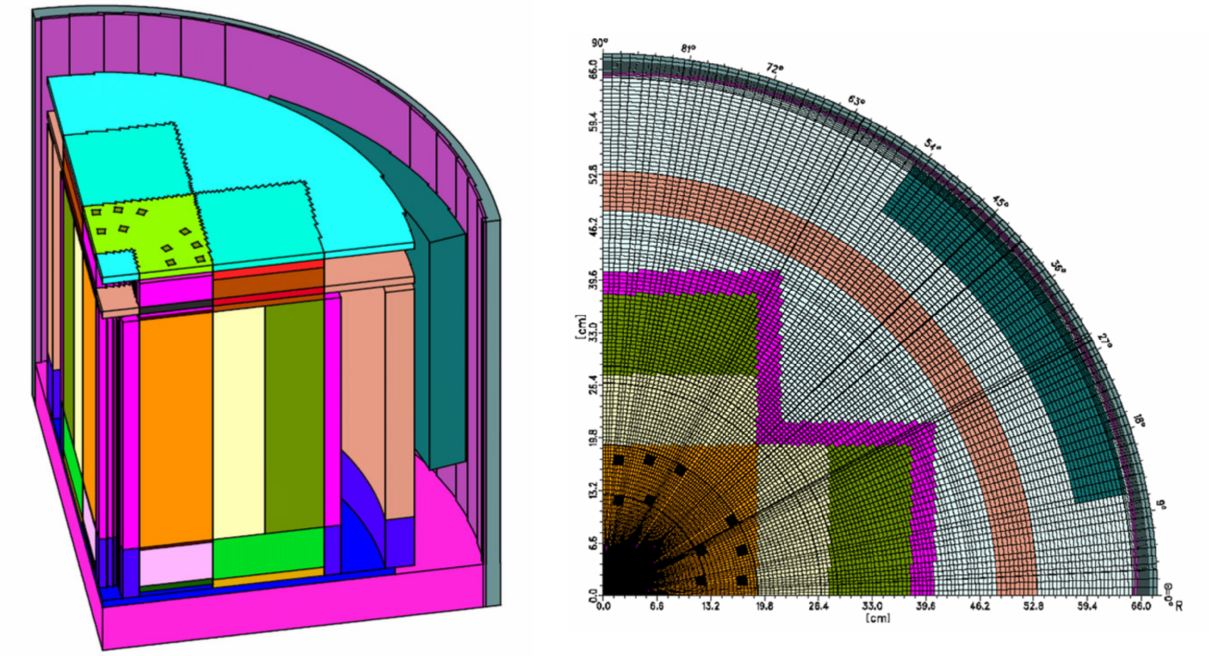

Figure 1. BOT3P model of the VENUS-2 (left) and a cross-section of the corresponding TORT mesh (right) at core mid-plane.

2.2.2. MultiTrans code

In the MultiTrans code, the simplified spherical harmonics approximation (SP_3) is used as a radiation transport approximation. The MultiTrans code has been developed at VTT for 3-D radiation transport problems. The adaptive tree multigrid technique enables local refinement of the calculation grid combined with the use of effective multigrid acceleration on tree-structured nested grids: starting from a fast solution on coarse grid, successive solutions are obtained on finer and finer grids. The method has been outlined in more detail elsewhere [3–5]. However, it is worth mentioning that the used SP_3 approximation has certain limitations. For a valid SP_3 approximation, the physical system should be thick enough so that the probability for neutrons to leak out is small (less than 0.5). In addition, the absorption probability should not be too high (also less than 0.5) and the mean scattering cosine should not be too close to unity. In other words, when the transport solution behaves diffusion-like, the SP_3 approximation should produce good results, but when the solution is very transport-like (streaming etc.) the results are expected to be inaccurate.

For the MultiTrans code, the geometry was constructed by using commercial CAD software, and the tree multigrid (octree grid) was generated from the exported stereolitography (STL) files, resulting in 2530817 octree cells (2204715 leaf cells, i.e. cells that are not divided further). The CAD model and the horizontal MultiTrans mesh at core mid-plane are shown in Figure 2.

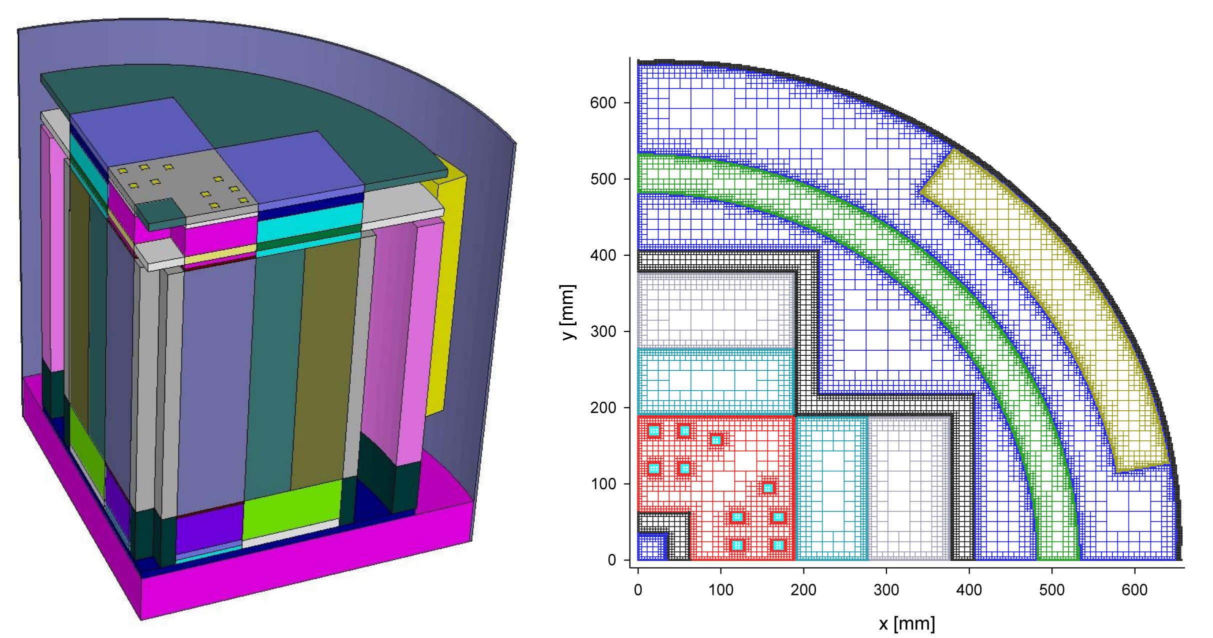

Figure 2. CAD model of the VENUS-2 (left) and a cross-section of the corresponding tree multigrid (right) at core mid-plane.

The running time for a MultiTrans criticality calculation was 16.0 hours on a desktop PC running Windows XP with 3.0 GHz P4 processor.

2.3. Calculations with the Stochastic Monte Carlo Code MCNP

The stochastic Monte Carlo transport calculations were performed by MCNP4C, using cross-sections from the endf60 library (.60c) based on ENDF/B-VI and released together with MCNP4C. The geometry was modelled according to the benchmark specifications (Figures 4 and 5 in the appendix of [6]). The isotopic compositions of actinides were also taken from the benchmark specifications. Otherwise natural element cross sections were used where available in endf60. Where they were not available, the full isotopic compositions given in the nuclide chart published by the Japanese Nuclear Data Committee in 1992 were used for Cr and heavier elements, but for H, N and O minor isotopes were ignored on the basis that they were present only in negligible amounts, except for ^{18}O, which is not included in endf60 anyway.

Two different sources were used: a KCODE source calculated by MCNP4C itself and the fixed source given in the benchmark specifications.

In the KCODE calculations, a constant starting source, equal everywhere in the core, was used. 200 inactive cycles were run, followed by 2,000 active cycles, each of 5,000 starters. k_{eff} was calculated to be 0.99857 with an estimated standard deviation of 0.00026. There was no indication that the number of inactive cycles was insufficient, and for such a small core and a flat starting source there was also no reason to suppose that more would have been needed.

In the fixed source calculations, module ‘four’ of the source preparation program PVIS-4 [12] was used to make a Fourier transform of the given distribution and to extend this to the full pin length. The source distribution was set equal to the fission rate distribution given in the specifications. This was not correct, since ν is higher for MOX fuel than for ^{235}U, but the extra work it would have taken to adjust the distribution to account for this was considered impracticable. However, in calculating the normalization factor for source strength the correct ν value for thermal fission was determined. For ^{235}U we used the thermal ν value given by Mughabghab et al., i.e., 2.425 (the Monte Carlo calculations were done independently and thus slightly different values were used than in calculations with deterministic codes). In the MOX fuel, the ν values (2.877 for ^{239}Pu and 2.937 for ^{241}Pu) were weighted with the number densities and thermal fission cross sections of each isotope, giving an average ν of 2.695. The respective ν values for pure UO_2 fuel and MOX fuel were then weighted with the fission rates in the respective parts of the core, giving an overall average of 2.485. This was then used to multiply the total fission rate, giving a total source in one quadrant of 1.142E13 s-1. Taking ν values for fast fission into account would have required a full spectrum calculation, which was deemed impracticable. At least the different fission spectra for different nuclides were taken into account.

The induced fission rate distribution was tallied using an F4 tally multiplied by the fission cross section. The distributions for the fixed source and KCODE calculations were significantly different. In the KCODE calculation, the fission rate was higher in the MOX fuel, by 10 % or sometimes more near the outer edge, and lower in the UO_2 fuel. This is in fact reasonable, considering the neglect of the difference in ν for different fuels in the fixed source distribution. Thus it seems likely that the KCODE results may be more accurate.

To reduce the variance, a mild importance biasing was used. Importancies were set to 0.5 or less above and below the core and to 2 in the outer baffle and reflector in the range 105 cm $< z <$ 155 cm, to 4 in the water gap and neutron pad, then decreasing back to 2 in the jacket inner wall and to 1 beyond that.

The dosimetry cross sections were taken from IRDF-90 version 2 library given in the 640-group SAND-II scheme. This group structure is sufficiently fine that one would expect the reaction rates to be effectively equivalent to what continuous energy data would give, unless some resonances in the dosimeters and the ambient materials nearly coincide.

3. RESULTS

The equivalent fission fluxes at 100 % power in the stainless steel zones calculated by TORT, MultiTrans and MCNP are given in Tables II-IV. The equivalent fission fluxes in the water zones are given in Tables V-VII, respectively.

Table II. TORT equivalent fission fluxes in stainless steel zones: neutrons/cm^2/sec

Measurement Position [1)]	^{58}Ni(n,p)	^{115}In(n,n')	^{103}Rh(n,n')	^{64}Zn(n,p)	^{237}Np(n,f)	^{27}Al(n,α)	Flux at E>0.1MeV	Flux at E>1.0MeV
Inner Baffle								
(-4.41, -0.63)	1.56 10^9	1.98 10^9	2.40 10^9	1.51 10^9	2.65 10^9	1.40 10^9	3.60 10^9	1.49 10^9
(-4.41, -4.41)	1.79 10^9	2.26 10^9	2.73 10^9	1.73 10^9	3.01 10^9	1.60 10^9	4.06 10^9	1.71 10^9
Outer Baffle								
(-39.69, -0.69)	5.15 10^8	6.36 10^8	7.54 10^8	4.99 10^8	8.26 10^8	4.69 10^8	1.10 10^9	4.75 10^8
(-39.69, -5.67)	4.79 10^8	5.92 10^8	7.05 10^8	4.63 10^8	7.73 10^8	4.35 10^8	1.03 10^9	4.43 10^8
(-39.69, -11.97)	3.82 10^8	4.74 10^8	5.65 10^8	3.69 10^8	6.20 10^8	3.49 10^8	8.27 10^8	3.54 10^8
(-39.69, -18.27)	2.15 10^8	2.71 10^8	3.29 10^8	2.07 10^8	3.64 10^8	2.00 10^8	4.94 10^8	2.04 10^8
(-37.17, -20.79)	2.38 10^8	3.01 10^8	3.66 10^8	2.29 10^8	4.05 10^8	2.22 10^8	5.51 10^8	2.27 10^8
(-30.87, -20.79)	5.35 10^8	6.69 10^8	8.03 10^8	5.16 10^8	8.83 10^8	4.83 10^8	1.19 10^9	5.02 10^8
(-24.57, -20.79)	8.08 10^8	1.02 10^9	1.24 10^9	7.79 10^8	1.37 10^9	7.16 10^8	1.87 10^9	7.72 10^8
Barrel								
(-49.77, -0.63)	6.34 10^7	7.50 10^7	8.79 10^7	6.11 10^7	9.70 10^7	7.15 10^7	1.26 10^8	5.60 10^7
(-49.77, -9.45)	5.18 10^7	6.41 10^7	7.74 10^7	4.96 10^7	8.60 10^7	5.69 10^7	1.16 10^8	4.86 10^7
(-47.25, -18.27)	5.09 10^7	6.50 10^7	8.03 10^7	4.86 10^7	8.99 10^7	5.41 10^7	1.24 10^8	4.97 10^7
(-45.99, -22.05)	4.59 10^7	6.04 10^7	7.62 10^7	4.36 10^7	8.59 10^7	4.78 10^7	1.21 10^8	4.66 10^7
(-44.73, -24.57)	4.17 10^7	5.48 10^7	6.90 10^7	3.97 10^7	7.77 10^7	4.40 10^7	1.10 10^8	4.22 10^7
(-42.21, -28.35)	3.79 10^7	4.73 10^7	5.81 10^7	3.63 10^7	6.48 10^7	4.34 10^7	8.89 10^7	3.60 10^7
(-38.43, -33.39)	3.40 10^7	3.94 10^7	4.64 10^7	3.28 10^7	5.09 10^7	4.32 10^7	6.66 10^7	2.95 10^7
(-35.91, -35.91)	3.34 10^7	3.84 10^7	4.51 10^7	3.22 10^7	4.93 10^7	4.29 10^7	6.42 10^7	2.87 10^7
Neutron Pad								
(-58.54, -22.47)	5.05 10^6	6.42 10^6	8.13 10^6	4.79 10^6	9.12 10^6	6.81 10^6	1.29 10^7	4.98 10^6
(-46.60, -41.95)	3.95 10^6	4.80 10^6	6.01 10^6	3.76 10^6	6.70 10^6	5.90 10^6	9.37 10^6	3.70 10^6

[1)] (x,y) in [cm,cm] co-ordinates with respect to core center

Table III. MultiTrans equivalent fission fluxes in stainless steel zones: neutrons/cm^2/sec

Measurement Position [1)]	^{58}Ni(n,p)	^{115}In(n,n')	^{103}Rh(n,n')	^{64}Zn(n,p)	^{237}Np(n,f)	^{27}Al(n,α)	Flux at E>0.1MeV	Flux at E>1.0MeV
Inner Baffle								
(-4.41, -0.63)	1.50 10^9	1.83 10^9	2.18 10^9	1.46 10^9	2.40 10^9	1.43 10^9	3.22 10^9	1.37 10^9
(-4.41, -4.41)	2.02 10^9	2.38 10^9	2.77 10^9	1.97 10^9	3.01 10^9	1.92 10^9	3.94 10^9	1.76 10^9
Outer Baffle								
(-39.69, -0.69)	5.25 10^8	6.32 10^8	7.43 10^8	5.09 10^8	8.11 10^8	4.93 10^8	1.08 10^9	4.69 10^8

(-39.69, -5.67)	$5.12\ 10^{8}$	$6.12\ 10^{8}$	$7.16\ 10^{8}$	$4.98\ 10^{8}$	$7.79\ 10^{8}$	$4.84\ 10^{8}$	$1.03\ 10^{9}$	$4.52\ 10^{8}$
(-39.69, -11.97)	$4.19\ 10^{8}$	$5.01\ 10^{8}$	$5.87\ 10^{8}$	$4.07\ 10^{8}$	$6.39\ 10^{8}$	$3.97\ 10^{8}$	$8.47\ 10^{8}$	$3.70\ 10^{8}$
(-39.69, -18.27)	$2.43\ 10^{8}$	$2.98\ 10^{8}$	$3.56\ 10^{8}$	$2.35\ 10^{8}$	$3.91\ 10^{8}$	$2.33\ 10^{8}$	$5.30\ 10^{8}$	$2.22\ 10^{8}$
(-37.17, -20.79)	$2.62\ 10^{8}$	$3.15\ 10^{8}$	$3.74\ 10^{8}$	$2.54\ 10^{8}$	$4.11\ 10^{8}$	$2.55\ 10^{8}$	$5.50\ 10^{8}$	$2.34\ 10^{8}$
(-30.87, -20.79)	$5.44\ 10^{8}$	$6.49\ 10^{8}$	$7.62\ 10^{8}$	$5.29\ 10^{8}$	$8.34\ 10^{8}$	$5.18\ 10^{8}$	$1.10\ 10^{9}$	$4.81\ 10^{8}$
(-24.57, -20.79)	$9.47\ 10^{8}$	$1.14\ 10^{9}$	$1.35\ 10^{9}$	$9.19\ 10^{8}$	$1.48\ 10^{9}$	$8.85\ 10^{8}$	$1.97\ 10^{9}$	$8.48\ 10^{8}$
Barrel								
(-49.77, -0.63)	$5.95\ 10^{7}$	$6.60\ 10^{7}$	$7.52\ 10^{7}$	$5.80\ 10^{7}$	$8.15\ 10^{7}$	$7.09\ 10^{7}$	$1.03\ 10^{8}$	$4.85\ 10^{7}$
(-49.77, -9.45)	$5.11\ 10^{7}$	$5.89\ 10^{7}$	$6.88\ 10^{7}$	$4.95\ 10^{7}$	$7.54\ 10^{7}$	$5.95\ 10^{7}$	$9.83\ 10^{7}$	$4.38\ 10^{7}$
(-47.25, -18.27)	$5.07\ 10^{7}$	$6.12\ 10^{7}$	$7.37\ 10^{7}$	$4.89\ 10^{7}$	$8.16\ 10^{7}$	$5.67\ 10^{7}$	$1.10\ 10^{8}$	$4.60\ 10^{7}$
(-45.99, -22.05)	$4.40\ 10^{7}$	$5.38\ 10^{7}$	$6.57\ 10^{7}$	$4.23\ 10^{7}$	$7.31\ 10^{7}$	$4.96\ 10^{7}$	$1.01\ 10^{8}$	$4.07\ 10^{7}$
(-44.73, -24.57)	$4.09\ 10^{7}$	$4.98\ 10^{7}$	$6.08\ 10^{7}$	$3.94\ 10^{7}$	$6.76\ 10^{7}$	$4.70\ 10^{7}$	$9.30\ 10^{7}$	$3.76\ 10^{7}$
(-42.21, -28.35)	$3.69\ 10^{7}$	$4.25\ 10^{7}$	$5.06\ 10^{7}$	$3.57\ 10^{7}$	$5.56\ 10^{7}$	$4.54\ 10^{7}$	$7.44\ 10^{7}$	$3.17\ 10^{7}$
(-38.43, -33.39)	$3.10\ 10^{7}$	$3.33\ 10^{7}$	$3.83\ 10^{7}$	$3.02\ 10^{7}$	$4.14\ 10^{7}$	$4.16\ 10^{7}$	$5.35\ 10^{7}$	$2.44\ 10^{7}$
(-35.91, -35.91)	$3.08\ 10^{7}$	$3.26\ 10^{7}$	$3.72\ 10^{7}$	$3.01\ 10^{7}$	$4.00\ 10^{7}$	$4.20\ 10^{7}$	$5.11\ 10^{7}$	$2.38\ 10^{7}$
Neutron Pad								
(-58.54, -22.47)	$4.72\ 10^{6}$	$5.35\ 10^{6}$	$6.43\ 10^{6}$	$4.54\ 10^{6}$	$7.04\ 10^{6}$	$7.17\ 10^{6}$	$9.32\ 10^{6}$	$4.04\ 10^{6}$
(-46.60, -41.95)	$3.46\ 10^{6}$	$3.72\ 10^{6}$	$4.43\ 10^{6}$	$3.35\ 10^{6}$	$4.83\ 10^{6}$	$5.95\ 10^{6}$	$6.37\ 10^{6}$	$2.79\ 10^{6}$

1) (x,y) in [cm,cm] co-ordinates with respect to core center

Table IV. MCNP equivalent fission fluxes in stainless steel zones: neutrons/cm^2/sec

Measurement Position 1)	^{58}**Ni(n,p)**	^{115}**In(n,n')**	^{103}**Rh(n,n')**	^{64}**Zn(n,p)**	^{237}**Np(n,f)**	^{27}**Al(n,α)**	**Flux at E>0.1MeV**	**Flux at E>1.0MeV**
Inner Baffle								
(-4.41, -0.63)	$1.28\ 10^{9}$	$1.63\ 10^{9}$	$1.97\ 10^{9}$	$1.24\ 10^{9}$	$2.17\ 10^{9}$	$1.19\ 10^{9}$	$2.92\ 10^{9}$	$1.21\ 10^{9}$
(-4.41, -4.41)	$1.70\ 10^{9}$	$2.14\ 10^{9}$	$2.53\ 10^{9}$	$1.64\ 10^{9}$	$2.78\ 10^{9}$	$1.48\ 10^{9}$	$3.72\ 10^{9}$	$1.56\ 10^{9}$
Outer Baffle								
(-39.69, -0.69)	$5.23\ 10^{8}$	$6.44\ 10^{8}$	$7.72\ 10^{8}$	$5.06\ 10^{8}$	$8.45\ 10^{8}$	$4.95\ 10^{8}$	$1.11\ 10^{9}$	$4.85\ 10^{8}$
(-39.69, -5.67)	$5.20\ 10^{8}$	$6.51\ 10^{8}$	$7.73\ 10^{8}$	$5.03\ 10^{8}$	$8.46\ 10^{8}$	$5.03\ 10^{8}$	$1.12\ 10^{9}$	$4.82\ 10^{8}$
(-39.69, -11.97)	$4.35\ 10^{8}$	$5.34\ 10^{8}$	$6.38\ 10^{8}$	$4.20\ 10^{8}$	$7.01\ 10^{8}$	$4.30\ 10^{8}$	$9.29\ 10^{8}$	$3.95\ 10^{8}$
(-39.69, -18.27)	$2.50\ 10^{8}$	$3.15\ 10^{8}$	$3.94\ 10^{8}$	$2.40\ 10^{8}$	$4.34\ 10^{8}$	$2.61\ 10^{8}$	$5.87\ 10^{8}$	$2.44\ 10^{8}$
(-37.17, -20.79)	$2.64\ 10^{8}$	$3.32\ 10^{8}$	$4.04\ 10^{8}$	$2.54\ 10^{8}$	$4.46\ 10^{8}$	$2.92\ 10^{8}$	$6.02\ 10^{8}$	$2.49\ 10^{8}$
(-30.87, -20.79)	$5.23\ 10^{8}$	$6.48\ 10^{8}$	$7.81\ 10^{8}$	$5.06\ 10^{8}$	$8.59\ 10^{8}$	$5.57\ 10^{8}$	$1.14\ 10^{9}$	$4.84\ 10^{8}$
(-24.57, -20.79)	$8.29\ 10^{8}$	$1.05\ 10^{9}$	$1.25\ 10^{9}$	$8.00\ 10^{8}$	$1.38\ 10^{9}$	$7.76\ 10^{8}$	$1.85\ 10^{9}$	$7.75\ 10^{8}$
Barrel								
(-49.77, -0.63)	$6.55\ 10^{7}$	$7.81\ 10^{7}$	$9.10\ 10^{7}$	$6.32\ 10^{7}$	$1.00\ 10^{8}$	$8.07\ 10^{7}$	$1.28\ 10^{8}$	$5.75\ 10^{7}$

(-49.77, -9.45)	6.01 10^{7}	7.43 10^{7}	9.02 10^{7}	5.76 10^{7}	1.00 10^{8}	6.53 10^{7}	1.32 10^{8}	5.67 10^{7}
(-47.25, -18.27)	5.86 10^{7}	7.51 10^{7}	9.31 10^{7}	5.59 10^{7}	1.04 10^{8}	5.76 10^{7}	1.39 10^{8}	5.73 10^{7}
(-45.99, -22.05)	4.99 10^{7}	6.48 10^{7}	8.03 10^{7}	4.73 10^{7}	9.06 10^{7}	6.35 10^{7}	1.26 10^{8}	4.82 10^{7}
(-44.73, -24.57)	4.36 10^{7}	5.75 10^{7}	7.25 10^{7}	4.15 10^{7}	8.20 10^{7}	4.85 10^{7}	1.11 10^{8}	4.42 10^{7}
(-42.21, -28.35)	3.96 10^{7}	5.02 10^{7}	5.94 10^{7}	3.77 10^{7}	6.64 10^{7}	5.20 10^{7}	9.01 10^{7}	3.66 10^{7}
(-38.43, -33.39)	3.41 10^{7}	4.04 10^{7}	4.81 10^{7}	3.28 10^{7}	5.29 10^{7}	4.38 10^{7}	6.90 10^{7}	3.07 10^{7}
(-35.91, -35.91)	3.50 10^{7}	3.99 10^{7}	4.80 10^{7}	3.37 10^{7}	5.30 10^{7}	4.25 10^{7}	6.79 10^{7}	3.09 10^{7}
Neutron Pad								
(-58.54, -22.47)	5.89 10^{6}	7.42 10^{6}	9.39 10^{6}	5.60 10^{6}	1.06 10^{7}	7.38 10^{6}	1.47 10^{7}	5.78 10^{6}
(-46.60, -41.95)	4.16 10^{6}	5.07 10^{6}	6.84 10^{6}	3.95 10^{6}	7.60 10^{6}	6.44 10^{6}	1.06 10^{7}	4.11 10^{6}

[1)] (x,y) in [cm,cm] co-ordinates with respect to core center

Table V. TORT equivalent fission fluxes in water zones: neutrons/cm^2/sec

Measurement Position [1)]	**^{58}Ni(n,p)**	**^{115}In(n,n')**	**^{103}Rh(n,n')**	**^{64}Zn(n,p)**	**^{237}Np(n,f)**	**^{27}Al(n,α)**	**Flux at E>0.1MeV**	**Flux at E>1.0MeV**
Central Hole								
(00.00, 00.00)	1.11 10^{9}	1.25 10^{9}	1.42 10^{9}	1.08 10^{9}	1.58 10^{9}	1.14 10^{9}	2.02 10^{9}	9.06 10^{8}
Water Gap								
(-54.36, -9.59)	2.02 10^{7}	2.24 10^{7}	2.61 10^{7}	1.96 10^{7}	2.97 10^{7}	2.63 10^{7}	3.78 10^{7}	1.65 10^{7}
(-52.89, -15.80)	2.01 10^{7}	2.27 10^{7}	2.67 10^{7}	1.95 10^{7}	3.08 10^{7}	2.57 10^{7}	3.97 10^{7}	1.68 10^{7}
(-51.53, -19.78)	1.95 10^{7}	2.23 10^{7}	2.64 10^{7}	1.89 10^{7}	3.05 10^{7}	2.48 10^{7}	3.97 10^{7}	1.65 10^{7}
(-50.03, -23.33)	1.75 10^{7}	2.05 10^{7}	2.47 10^{7}	1.69 10^{7}	2.88 10^{7}	2.18 10^{7}	3.80 10^{7}	1.53 10^{7}
(-48.74, -25.91)	1.67 10^{7}	1.94 10^{7}	2.33 10^{7}	1.61 10^{7}	2.71 10^{7}	2.10 10^{7}	3.57 10^{7}	1.45 10^{7}
(-46.29, -30.06)	1.52 10^{7}	1.70 10^{7}	2.00 10^{7}	1.47 10^{7}	2.30 10^{7}	2.03 10^{7}	2.98 10^{7}	1.25 10^{7}
(-44.08, -33.22)	1.45 10^{7}	1.58 10^{7}	1.85 10^{7}	1.41 10^{7}	2.11 10^{7}	2.03 10^{7}	2.69 10^{7}	1.16 10^{7}
(-42.29, -35.48)	1.41 10^{7}	1.49 10^{7}	1.72 10^{7}	1.37 10^{7}	1.94 10^{7}	2.05 10^{7}	2.44 10^{7}	1.09 10^{7}
(-39.03, -39.03)	1.39 10^{7}	1.45 10^{7}	1.65 10^{7}	1.35 10^{7}	1.86 10^{7}	2.05 10^{7}	2.32 10^{7}	1.06 10^{7}
Reflector								
(-23.31, -23.31)	6.35 10^{8}	7.48 10^{8}	8.77 10^{8}	6.19 10^{8}	9.80 10^{8}	6.15 10^{8}	1.29 10^{9}	5.51 10^{8}
(-25.83, -25.83)	3.35 10^{8}	3.65 10^{8}	4.08 10^{8}	3.29 10^{8}	4.72 10^{8}	3.63 10^{8}	5.64 10^{8}	2.63 10^{8}
(-28.35, -28.35)	1.85 10^{8}	1.91 10^{8}	2.07 10^{8}	1.82 10^{8}	2.44 10^{8}	2.18 10^{8}	2.71 10^{8}	1.36 10^{8}
(-30.87, -30.87)	9.64 10^{7}	9.49 10^{7}	1.00 10^{8}	9.53 10^{7}	1.17 10^{8}	1.25 10^{8}	1.25 10^{8}	6.65 10^{7}
(-33.39, -33.39)	5.59 10^{7}	5.59 10^{7}	6.01 10^{7}	5.50 10^{7}	6.70 10^{7}	7.55 10^{7}	7.67 10^{7}	3.96 10^{7}

[1)] (x,y) in [cm,cm] co-ordinates with respect to core center

Table VI. MultiTrans equivalent fission fluxes in water zones: neutrons/cm^2/sec

Measurement Position [1)]	^{58}Ni(n,p)	^{115}In(n,n')	^{103}Rh(n,n')	^{64}Zn(n,p)	^{237}Np(n,f)	^{27}Al(n,α)	Flux at E>0.1MeV	Flux at E>1.0MeV
Central Hole								
(00.00, 00.00)	1.02 10^9	1.12 10^9	1.24 10^9	1.01 10^9	1.42 10^9	1.10 10^9	1.68 10^9	8.03 10^8
Water Gap								
(-54.36, -9.59)	1.99 10^7	2.18 10^7	2.51 10^7	1.94 10^7	2.81 10^7	2.59 10^7	3.56 10^7	1.59 10^7
(-52.89, -15.80)	1.94 10^7	2.14 10^7	2.50 10^7	1.88 10^7	2.82 10^7	2.49 10^7	3.60 10^7	1.57 10^7
(-51.53, -19.78)	1.89 10^7	2.14 10^7	2.52 10^7	1.83 10^7	2.86 10^7	2.41 10^7	3.71 10^7	1.58 10^7
(-50.03, -23.33)	1.76 10^7	1.95 10^7	2.27 10^7	1.71 10^7	2.59 10^7	2.30 10^7	3.28 10^7	1.43 10^7
(-48.74, -25.91)	1.72 10^7	1.93 10^7	2.29 10^7	1.67 10^7	2.60 10^7	2.25 10^7	3.40 10^7	1.43 10^7
(-46.29, -30.06)	1.60 10^7	1.77 10^7	2.09 10^7	1.55 10^7	2.34 10^7	2.17 10^7	3.06 10^7	1.31 10^7
(-44.08, -33.22)	1.41 10^7	1.48 10^7	1.70 10^7	1.37 10^7	1.90 10^7	2.03 10^7	2.40 10^7	1.08 10^7
(-42.29, -35.48)	1.35 10^7	1.39 10^7	1.59 10^7	1.32 10^7	1.75 10^7	1.99 10^7	2.21 10^7	1.01 10^7
(-39.03, -39.03)	1.29 10^7	1.29 10^7	1.45 10^7	1.27 10^7	1.59 10^7	1.96 10^7	1.96 10^7	9.27 10^6
Reflector								
(-23.31, -23.31)	6.94 10^8	8.20 10^8	9.59 10^8	6.75 10^8	1.07 10^9	6.77 10^8	1.39 10^9	6.04 10^8
(-25.83, -25.83)	3.78 10^8	4.22 10^8	4.80 10^8	3.70 10^8	5.43 10^8	3.98 10^8	6.71 10^8	3.06 10^8
(-28.35, -28.35)	2.01 10^8	2.10 10^8	2.30 10^8	1.98 10^8	2.63 10^8	2.33 10^8	3.03 10^8	1.50 10^8
(-30.87, -30.87)	1.02 10^8	9.86 10^7	1.03 10^8	1.02 10^8	1.17 10^8	1.32 10^8	1.25 10^8	6.86 10^7
(-33.39, -33.39)	5.38 10^7	5.01 10^7	5.24 10^7	5.35 10^7	5.66 10^7	7.60 10^7	6.28 10^7	3.48 10^7

[1)] (x,y) in [cm,cm] co-ordinates with respect to core center

Table VII. MCNP equivalent fission fluxes in water zones: neutrons/cm^2/sec

Measurement Position [1)]	^{58}Ni(n,p)	^{115}In(n,n')	^{103}Rh(n,n')	^{64}Zn(n,p)	^{237}Np(n,f)	^{27}Al(n,α)	Flux at E>0.1MeV	Flux at E>1.0MeV
Central Hole								
(00.00, 00.00)	1.05 10^9	1.19 10^9	1.37 10^9	1.02 10^9	1.54 10^9	1.10 10^9	1.94 10^9	8.69 10^8
Water Gap								
(-54.36, -9.59)	2.14 10^7	2.34 10^7	2.94 10^7	2.08 10^7	3.34 10^7	2.72 10^7	4.23 10^7	1.81 10^7
(-52.89, -15.80)	2.09 10^7	2.43 10^7	2.88 10^7	2.02 10^7	3.28 10^7	2.46 10^7	4.15 10^7	1.84 10^7
(-51.53, -19.78)	2.09 10^7	2.38 10^7	2.96 10^7	2.02 10^7	3.37 10^7	2.66 10^7	4.37 10^7	1.86 10^7
(-50.03, -23.33)	2.03 10^7	2.26 10^7	2.61 10^7	1.96 10^7	3.00 10^7	2.93 10^7	3.88 10^7	1.60 10^7
(-48.74, -25.91)	1.77 10^7	2.05 10^7	2.48 10^7	1.72 10^7	2.88 10^7	2.34 10^7	3.75 10^7	1.54 10^7
(-46.29, -30.06)	1.57 10^7	1.77 10^7	2.09 10^7	1.53 10^7	2.39 10^7	2.19 10^7	3.21 10^7	1.33 10^7
(-44.08, -33.22)	1.50 10^7	1.62 10^7	1.78 10^7	1.46 10^7	2.04 10^7	2.23 10^7	2.68 10^7	1.12 10^7

(-42.29, -35.48)	$1.44\ 10^{7}$	$1.54\ 10^{7}$	$1.82\ 10^{7}$	$1.40\ 10^{7}$	$2.04\ 10^{7}$	$1.97\ 10^{7}$	$2.51\ 10^{7}$	$1.16\ 10^{7}$
(-39.03, -39.03)	$1.40\ 10^{7}$	$1.47\ 10^{7}$	$1.57\ 10^{7}$	$1.37\ 10^{7}$	$1.77\ 10^{7}$	$2.27\ 10^{7}$	$2.24\ 10^{7}$	$1.00\ 10^{7}$
Reflector								
(-23.31, -23.31)	$6.12\ 10^{8}$	$7.21\ 10^{8}$	$8.26\ 10^{8}$	$5.95\ 10^{8}$	$9.19\ 10^{8}$	$6.55\ 10^{8}$	$1.20\ 10^{9}$	$5.14\ 10^{8}$
(-25.83, -25.83)	$3.33\ 10^{8}$	$3.64\ 10^{8}$	$4.09\ 10^{8}$	$3.27\ 10^{8}$	$4.63\ 10^{8}$	$3.66\ 10^{8}$	$5.58\ 10^{8}$	$2.60\ 10^{8}$
(-28.35, -28.35)	$1.83\ 10^{8}$	$1.90\ 10^{8}$	$2.04\ 10^{8}$	$1.80\ 10^{8}$	$2.36\ 10^{8}$	$2.16\ 10^{8}$	$2.69\ 10^{8}$	$1.32\ 10^{8}$
(-30.87, -30.87)	$1.06\ 10^{8}$	$1.04\ 10^{8}$	$1.06\ 10^{8}$	$1.04\ 10^{8}$	$1.24\ 10^{8}$	$1.46\ 10^{8}$	$1.35\ 10^{8}$	$6.90\ 10^{7}$
(-33.39, -33.39)	$6.15\ 10^{7}$	$6.07\ 10^{7}$	$6.62\ 10^{7}$	$6.03\ 10^{7}$	$7.50\ 10^{7}$	$8.89\ 10^{7}$	$8.39\ 10^{7}$	$4.37\ 10^{7}$

[1)] (x,y) in [cm,cm] co-ordinates with respect to core center

3. DISCUSSION AND CONCLUSIONS

The agreement between TORT and MCNP results was rather good: 75 % of the reported values agreed within 10 % and 96 % of the values were within 20 %. Over 20 % disagreement in fission flux values for reactions other than $^{27}Al(n,\alpha)$ was found in one detector position inside the inner baffle. In other detector positions only some fission flux values of $^{27}Al(n,\alpha)$ reaction disagreed more than 20 %. The maximum difference between TORT and MCNP results was 26 % for fission flux values of $^{27}Al(n,\alpha)$ reaction inside the water gap.

A very large discrepancy in the calculated values was found between MultiTrans and other two codes inside the neutron pad: the maximum difference in the E > 0.1 MeV flux was 28 % and 32 % in 2 detector positions compared to TORT, and 36 % and 40 % compared to MCNP, respectively. The disagreement inside the neutron pad was to some extent anticipated due to approximative radiation transport method (SP_3) which does not produce accurate results when the solution behaves more transport-like. It seems that MultiTrans underestimates the fission fluxes not only in the neutron pad, but also to some extent in the barrel region. The MultiTrans results agreed better with TORT than with MCNP. Over 20 % discrepancies between MultiTrans and TORT results were found, in addition to the neutron pad, only in one detector position for the E > 0.1 MeV flux inside the barrel, and for $^{27}Al(n,\alpha)$ fission flux in one detector positions inside the inner and outer baffles.

The results given in this paper are the very same as the values submitted to NEA. The measured values are at the moment not yet open to the participants, and therefore a comparative analysis between the calculated and measured values will remain as a future work.

ACKNOWLEDGMENTS

This work was performed within the EMERALD project of the national SAFIR research programme.

REFERENCES

1. J. F. Briesmeister (Ed.), “MCNP—A General Monte Carlo N-Particle Transport Code, Version 4C,” Los Alamos National Laboratory, LA-13709-M (2000).
2. W. A. Rhoades, D. B. Simpson, “The TORT Three-Dimensional Discrete Ordinates Neutron/Photon Transport Code (TORT Version 3),” Oak Ridge National Laboratory, ORNL/TM-13221 (1997).
3. P. Kotiluoto, “Fast Tree Multigrid Transport Application for the Simplified P_3 Approximation,” *Nucl. Sci. Eng.*, **138**, pp. 269–278 (2001).
4. P. Kotiluoto, P. Hiismäki, S. Savolainen, “Application of the New MultiTrans SP_3 Radiation Transport Code in BNCT Dose Planning,” *Med. Phys.*, **28**, pp. 1905–1910 (2001).
5. P. Kotiluoto, “Application of the New MultiTrans SP_3 Radiation Transport Code in Criticality Problems and Potential Use in Dosimetry,” *Proceedings of the 11th International Symposium on Reactor Dosimetry*, Brussels, Belgium, 18-23 August 2002, In: *Reactor Dosimetry in the 21st Century*, World Scientific, Singapore, pp. 580–587 (2003).
6. C. Y. Han, C.-H. Shin, H.-C. Kim, J. K. Kim, N. Messaoudi, B.-C. Na, “VENUS-2 MOX-fuelled Reactor Dosimetry Calculations, Benchmark Specification,” Nuclear Energy Agency, NEA/NSC/DOC(2004)6.
7. J. E. White, D. T. Ingersoll, R. Q. Wright, *et al.*, “Production and Testing of the Revised VITAMIN-B6 Fine-Group and the BUGLE-96 Broad-Group Neutron/Photon Cross-Section Libraries,” Oak Ridge National Laboratory, ORNL-6795, NUREG/CR-6214, Rev. 1 (1995).
8. F. Wasastjerna, ”TOPICS-B. A Batch Version of the Cross Section Preparation Program TOPICS,” VTT Energy, Programme Document ENE4-PD-5/01 (2001).
9. É. M. Zsolnay, E. J. Szondi, H. J. Nolthenius, “The Neutron Metrology File NMF-90,” IAEA-NDS-171, Rev. 1 (1999).
10. R. Orsi, “BOT3P: Bologna Transport Analysis Pre-Post-processors Version 3.0,” *Nucl. Sci. Eng.*, **146**, pp. 248–255 (2004).
11. R. Orsi, “BOT3P Version 3.0: The ENEA Bologna Pre-Processors of the DORT, TORT, TWODANT, THREEDANT and MCNP Transport Codes and Post-Processors of DORT and TORT,“ ENEA, FIS-P129-001 (2002).
12. F. Wasastjerna, “PVIS-4 – A Program Intended to Prepare a Fixed Fission Source for Pressure Vessel Irradiation Calculations with ANISN, DORT or TORT in Hexagonal or Square Geometry,” VTT Energy Technical Report RFD-2/99 (1999).